Increased lethality in Influenza and SARS-CoV-2 co-infection is prevented by influenza immunity but not SARS-CoV-2 immunity

Hagit Achdout
Israel Institute for Biological Research
Einat B. Vitner
Israel Institute for Biological Research https://orcid.org/0000-0001-8578-8551
Boaz Politi
Israel Institute for Biological Research
Sharon Melamed
Israel Institute for Biological Research
Yfat Yahalom-Ronen
Israel Institute for Biological Research
Hadas Tamir
Israel Institute for Biological Research
Noam Erez
Israel Institute for Biological Research
Roy Avraham
Israel Institute for Biological Research
Lilach Cherry
Israel Institute for Biological Research
Efi Makdasi
Israel Institute for Biological Research
Didi Gur
Israel Institute for Biological Research
Moshe Aftalion
Israel Institute for Biological Research
Yaron Vagima
Israel Institute for Biological Research
Nir Paran
Israel Institute for Biological Research https://orcid.org/0000-0001-5143-9660
Tomer Israely (tomeri@iibr.gov.il)
Israel Institute for Biological Research https://orcid.org/0000-0003-0246-4477

Letter

Keywords: SARS-CoV-2, influenza, vaccination, lethality

Posted Date: January 13th, 2021

DOI: https://doi.org/10.21203/rs.3.rs-136702/v1

Version of Record: A version of this preprint was published at Nature Communications on October 5th, 2021. See the published version at https://doi.org/10.1038/s41467-021-26113-1.

Increased lethality in Influenza and SARS-CoV-2 co-infection is prevented by influenza immunity but not SARS-CoV-2 immunity

Hagit Achdout[1]*, Einat. B. Vitner[1*], Boaz Politi[1*], Sharon Melamed[1*], Yfat Yahalom-Ronen[1], Hadas Tamir[1], Noam Erez[1], Roy Avraham[1], Lilach Cherry[1], Efi Makdasi[1], Didi Gur[2], Moshe Aftalion[2], Yaron Vagima[2], Nir Paran[1], Tomer Israely[1¶]

Affiliations:

[1]Departments of Infectious diseases, Israel institute for Biological Research, Ness-Ziona, 7410001, Israel

[2]Department of Biochemistry and Molecular Genetics, Israel Institute for Biological Research, Ness-Ziona, 7410001, Israel.

*These authors contributed equally to this work

¶To whom correspondence should be addressed: tomeri@iibr.gov.il

Abstract

Severe acute respiratory syndrome coronavirus 2 (SARS-CoV-2) is the cause for the ongoing COVID-19 pandemic[1]. The continued spread of SARS-CoV-2 along with the imminent flu season increase the probability of influenza-SARS-CoV-2 dual infection which might result in a severe disease. In this study, we examined the disease outcome of influenza A virus (IAV) and SARS-CoV-2 co-infection in K18-hACE2 mice. Our data indicates that IAV-infected mice are more susceptible to develop severe disease upon co-infection with SARS-CoV-2 two days post influenza infection. This co-infection results in severe morbidity and nearly uniform fatality as compared to the non-fatal influenza disease, or the partial fatality of SARS-CoV-2 alone. Co-infection was associated with elevated influenza viral load in respiratory organs. Remarkably, prior immunity to influenza, but not to SARS-CoV-2, prevented the severe disease and mortality. These data provide an experimental support that flu intervention by prior vaccination may be valuable in reducing the risk of sever Flu - SARS-CoV-2 comorbidity, and highlight the importance of vaccination.

Main

COVID-19 pandemic presents with a broad spectrum of severity ranging from asymptomatic presentation to severe pneumonia. Several risk factors for severe COVID-19 disease, such age, sex, and obesity were identified[2]. Whether co-infection with other pathogens may impact disease severity, are yet to be elucidated. IAV infection is one of the leading causes of respiratory infections in the United States resulting in respiratory illness[3]. Complications involving secondary infections with pathogens, mostly bacteria, significantly exacerbate the risk of severe flu disease[4,5]. However, while most of the research in the field of secondary infections following IVA involves bacteria, the secondary effect of infection with viruses is a less explored area.

To delineate the interplay between IAV and SARS-CoV-2 infections, we employed transgenic mice expressing human angiotensin-converting enzyme 2 (hACE2) by the human cytokeratin 18 promoter (K18-hACE2) which represent a susceptible SARS-CoV-2 murine model[6]. Mice were infected with a non-lethal dose of mouse adapted IAV (A/Puerto Rico/8/1934 H1N1 (PR8)) and were subsequently infected with SARS-CoV-2 to mimic co-infection. While the terms 'co-infection' and 'superinfection' are often interchanges, the use of 'co-infection' herein after refers to a sequential infection with 2 viruses within a very short time, with the second infection occurring prior to elimination of the first virus.

First, the outcome of SARS-CoV-2 infection was tested at two days post influenza infection (dpIi), a pre-symptomatic stage of flu. At this stage, mice does not present any manifestations but the viral titer of IAV in the lungs is high[7]. IAV-infected mice, started losing weight 5 dpIi and exhibited maximal morbidity at 9-10 dpIi (75% of initial body

weight) (Fig. 1a). At eleven dpIi mice began to gain weight, and returned to their initial body weight by 18 dpIi. Remarkably, mice infected with SARS-CoV-2 two days post IAV-infection, exhibited an earlier and increased weight loss compared to IAV infection alone. Moreover, all of the co-infected mice died by 5-7 days post SARS-CoV-2 infection (dpSi), compared to no-death or only 38% lethality of the IAV- and SARS-CoV-2 infected mice, respectively (Fig. 1b p****<0.0001).

Next, we tested co-infection with SARS-CoV-2 at five days post IAV infection; the early-symptomatic stages. IAV infected and co-infected mice started to lose weight at 6-7 dpIi (Fig. 1c). However, while the IAV infected mice reached maximal weight loss 8-9 dpIi (84% of initial weight), the co-infected mice continued to lose weight until 10 dpIi (73% of initial body weight). Also, the recovery period of the co-infected mice was prolonged compared to IAV infected mice. While IAV infected mice reached 91% of initial body weight at 10 dpIi and returned to their initial body weight by 11 dpIi, the co-infected mice reached 91% of initial body weight only 16 dpIi and returned to baseline weight only 22 dpIi (Fig. 1c). Moreover, co-infection of SARS-CoV-2 at 5 dpIi results in 70% lethality rate in comparison to 43% among mice infected with SARS-CoV-2 alone (p=0.08) (Fig. 1d).

Finally, we tested co-infection when SARS-CoV-2 was administered during late-symptomatic stage of flu disease, in which maximal morbidity was detected (8 dpIi, Fig. 1e,f). At this time point, IAV is effectively cleared from the lungs[7]. Interestingly, SARS-CoV-2 infection at 8 dpIi had no effect on the body weight of the mice, nor on their survival rate. These results suggest that co-infection per se (infection with SARS-CoV-2, whilst the IAV is still present in the organs) results in a more severe disease. This may result from

the adaptive immunity to IAV which already takes place at 8 dpIi that contributes in avoiding influenza-disease exacerbations.

In the human population, co-infection is more likely to occur during the asymptomatic period, when the patient does not feel sick and is still active. Also, at this stage, as represented by two dpIi, co-infection results in the most severe and fatal disease. Therefore, we chose to focus on this stage, and hereafter co-infection refers to infection with IAV followed by infection with SARS-CoV-2 two days later.

To correlate between increased morbidity and mortality observed in co-infected mice and viral load, SARS-CoV-2 PFU and IAV viral load were quantified in the lungs and nasal turbinates (Fig. 2a). A significant increase in IAV viral RNA was observed in the lungs (4.6 -fold increase) and in the nasal turbinates (11-fold increase) of co-infected mice compared to IAV- infected mice (Fig. 2b,c), which coincide with the exacerbated disease. In contrast, the level of SARS-CoV-2 was reduced in the co-infected mice compared to SARS-CoV-2- infected mice both in the lung and in the nasal turbinates (Fig. 2d,e), suggesting a significant role for IAV in the observed severe disease. This finding is in accordance with previous evidence of pathogenic competition between respiratory viruses, such as influenza and seasonal coronaviruses[8,9]. A possible explanation for the reduced SARS-CoV-2 viral load might be the induction of innate immune response activated by IAV infection prior to the infection with SARS-CoV-2, and inhibiting establishment of infection and replication[10,11,12]. It is yet unclear what mechanism allows IAV to evade such antiviral immunity. In addition to innate immunity mechanisms underlying the reduced SARS-CoV-2 viral load, IAV infection may also interfere with SARS-CoV-2 infection through super-infection exclusion. It is yet to be determined whether a mechanism similar

98 to that previously shown for inhibiting influenza super-infection by neuraminidase (NA) is
99 also applied here[13]. Notably, though SARS-CoV-2 viral load was reduced in the co-infected
100 mice, the remaining levels were sufficient to trigger the lethal outcome of the co-infection.

101 Taken together, these results suggest that the increased morbidity and mortality detected in
102 the co-infected mice are associated with higher levels of IAV in the respiratory system,
103 rather than that of SARS-CoV-2.

104 To elaborate on the host response to IAV, SARS-CoV-2, and co-infection of IAV and
105 SARS-CoV-2, we assessed the expression of immune-related genes in the lungs at 4 and 2
106 days post IAV and SARS-CoV-2 infection, respectively (Fig. 2a). Overall, in lungs of
107 SARS-CoV-2 infected mice, no alterations in mRNA levels of the tested genes were
108 observed compared to uninfected mice (Fig. 3), most likely due to low infection dose
109 (10pfu/mouse) and short time post infection (2 days). Upon infection with IAV, all of the
110 tested genes were over-expressed (Fig. 3). Remarkably, IAV and SARS-CoV-2 co-
111 infection resulted in a significantly higher elevation of gene expression compared to that
112 exhibited upon IAV infection alone, indicating a robust induction of the immune system
113 that may lead to the exacerbated disease.

114 Then, we examined whether pre-existing immunity to SARS-CoV-2 prevents the severe
115 manifestations of co-infected mice. Efficient immunity to SARS-CoV-2 was induced by
116 infection of mice with a non-lethal dose of SARS-CoV-2. This infection induced
117 neutralizing antibodies against SARS-CoV-2 (data not shown), and rescued mice from
118 SARS-CoV-2 challenge (Fig. 4a). However, while pre-existing immunity to SARS-CoV-
119 2 completely prevented the lethality caused by SARS-CoV-2 infection, amounting to 33%,
120 it had no effect on the morbidity and lethality caused by IAV and SARS-CoV-2 co-

121 infection (90% compared to 86% lethality in pre-existing SARS-CoV-2 immunity) (Fig.
122 4a,b). This data further supports the notion that the severe manifestations of the co-
123 infection are not the result of SARS-CoV-2 replication.
124 To determine whether pre-existing immunity to IAV can prevent the co-infection
125 manifestations, mice were vaccinated intramuscular (i.m.) with IAV 30 days prior to viral
126 infection with IAV and SARS-CoV-2. Pre-exposure to IAV alleviated morbidity observed
127 upon infection with IAV (Fig. 4d), and had no effect on the survival rate upon SARS-CoV-
128 2 infection (50% compared to 67% survival, respectively. Fig. 4c,d, p=0.64). Remarkably,
129 pre-existing immunity to IAV prevented the severe manifestations and fatality caused by
130 IAV and SARS-CoV-2 co-infection. Neither weight loss nor increased lethality were
131 detected in the co-infected mice that were vaccinated to IAV compared to co-infected mice
132 without immune background (Fig. 4 c,d). Altogether, our data suggest that IAV- SARS-
133 CoV-2 co-infection results in a severe and lethal disease in susceptible mice. Severe
134 manifestations are associated with robust induction of innate immunity and elevated IAV
135 viral load in the respiratory organs. Importantly, prior immunity to Flu but not to SARS-
136 CoV-2 prevented disease and death. Based on these results, we suggest that flu
137 intervention, by prior vaccination, may prove valuable in reducing the risk of severe Flu -
138 SARS-CoV-2 comorbidity.
139

Methods

Cells

Vero E6 (ATCC® CRL-1586TM) were obtained from the American Type Culture Collection (Summit Pharmaceuticals International, Japan). Madin-Darby Canine Kidney (MDCK) cells (ATCC® CCL-34™) were kindly provided by Dr. Michal Mandelboim (Central Virology Laboratory, Ministry of Health, Chaim Sheba Medical Center, Tel-Hashomer, Israel). Cells were maintained in Dulbecco's Modified Eagle's Medium (DMEM) supplemented with 10% fetal bovine serum (FBS), MEM non-essential amino acids, 2 nM L-Glutamine, 100 Units/ml Penicillin, 0.1 mg/ml streptomycin and 12.5 Units/ml Nystatin (Biological Industries, Israel). Cells were cultured at 37°C, 5% CO_2 at 95% air atmosphere.

Viruses

SARS-CoV-2, isolate Human 2019-nCoV ex China strain BavPat1/2020 was kindly provided by Prof. Dr. Christian Drosten (Charité, Berlin) through the European Virus Archive – Global (EVAg Ref-SKU: 026V-03883). Virus stocks were propagated (4 passages) and tittered on Vero E6 cells. The virus was stored at -80°C until use.

Strain A/Puerto Rico/8/1934 (H1N1) influenza A virus (IAV, PR8) was a kind gift from Dr. Michal Mandelboim. The virus was propagated in embryonated chicken eggs as previously described[14]. HAU was determined with chicken erythrocytes, and virus titers were determined by a plaque assay on MDCK cell monolayers. The virus was stored at -80°C until use.

Animal experiments

All animal experiments involving SARS-CoV-2 were conducted in a BSL3 facility. Treatment of animals was in accordance with regulations outlined in the U.S. Department of Agriculture (USDA) Animal Welfare Act and the conditions specified in the Guide for Care and Use of Laboratory Animals (National Institute of Health, 2011). Animal studies were approved by the local IIBR ethical committee for animal experiments (protocols number M-29-20, M-40-20 and M-41-20). Female K18-hACE2 transgenic mice (The Jackson Laboratory) 6-8 weeks old were maintained at 20−22°C and a relative humidity of 50 ± 10% on a 12hrs light/dark cycle. Animals were fed with commercial rodent chow (Koffolk Inc.) and provided with tap water ad libitum. Prior to infection, mice were kept in groups of 10. Mice were randomly assigned to experimental groups.

For infection, the viruses were diluted in phosphate buffered saline (PBS) supplemented with 2% FBS (Biological Industries, Israel). Anesthetized animals (Ketamine 75 mg/kg, Xylazine 7.5 mg/kg in PBS) were infected by 20µl intranasal (i.n.) instillation (PR8 80pfu/mouse, SARS-CoV-2 10pfu/mouse).

Animal's immunization: for SARS-CoV-2 immunization, i.n. instillation of 2pfu/mouse SARS-CoV-2 was performed. For IAV immunization, mice were vaccinated intramuscularly (i.m.) with 10^6pfu/mouse. Immunized mice were infected 30 days post immunization.

Determination of viral load in organs

Viral loads were determined at 2 days post SARS-CoV-2 infection, or 4 days post influenza infection. In the co-infected group, viral load was determined 4 days post IAV infection, which is 2 days post SARS-CoV-2 infection. Each group of mice included 10 mice. K18-

hACE2 mice were sacrificed, and lungs and nasal turbinates (n.t.) were harvested and stored in -80°C until further processing. Organs were processed for titration in 1.5 mL of ice-cold PBS as previously described[15]. Part of the processed tissue samples was used immediately for RNA extraction for IAV viral RNA determination and for gene expression, while the other part was kept in -80°C until further processing for viral titration (used for SARS-CoV-2 pfu).

SARS-CoV-2 viral load was determined using pfu assay[16]. Briefly, serial dilutions of extracted organs from mice infected with SARS-CoV-2 or co-infected with IAV and SARS-CoV-2, were prepared in MEM containing 2% FCS, and used to infect Vero E6 monolayers in duplicates (200µl/well). Plates were incubated for 1 hour at 37ºC to allow viral adsorption. Then, 2ml/well of overlay (MEM containing 2% FBS and 0.4% tragacanth (Merck, Israel)) was added to each well and plates were incubated at 37°C, 5% CO_2 for 48 hours. The media was then aspirated and the cells were fixed and stained with 1ml/well of crystal violet solution (Biological Industries, Israel). The number of plaques in each well was determined, and SARS-CoV-2 PFU (plaque forming unit) titer was calculated.

IAV viral RNA was determined using Real-time RT-PCR (see below).

Quantitative Real-Time RT-PCR

RNA was extracted by Viral RNA mini kit (Qiagen, Germany) as per manufacturesr's instructions. IAV viral RNA load in the lung and nasal turbinates (n.t.) were determined by qRT-PCR. Real-time RT-PCR was conducted with SensiFAST™ Probe Lo-ROX One-Step Kit (Bioline, 78005) and analyzed with the 7500 Real Time PCR System (Applied Biosystems). The PFU Equivalent per organ (pfuE/organ) were calculated from standard curve generated from virus stocks. qPCR primers and probes for the detection of PR8: PR8-PA-FW:

209 CGGTCCAAATTCCTGCTGA; PR8-PA-RW:CATTGGGTTCCTTCCATCCA; PR8-PA-Probe:
210 CCAAGTCATGAAGGAGAGGGAATACCGCT
211 Total RNA extracted from lungs of mice infected with IAV or SARS-CoV-2, or co-
212 infected, at 2 dpSi and 4 dpIi was used to measure differently-expressed genes by qRT-
213 PCR using the corresponding specific primers printed on 96 well plates (Custom TaqMan
214 Array Plates, Applied BiosystemsTM) as previously described[15]. Briefly, 1 microgram
215 cDNA was synthesized out of the RNA using Verso cDNA Synthesis Kit (Thermo Fisher
216 Scientific, Waltham, MA, USA) according to the manufacturer's instructions. Samples
217 were subjected to qPCR with TaqMan® Fast Advanced Master Mix (7500 Real Time PCR
218 System, Applied Biosystems, Thermo Fisher Scientific). The housekeeping gene gapdh
219 was used to normalize fold change of each gene as compared to mock-infected control at
220 the same time point and was calculated as ΔΔCT.
221

Acknowledgment

The authors would like to thank Prof. Dr. Christian at the Charité Universitätsmedizin, Institute of Virology, Berlin, Germany for providing the SARS-CoV-2 BavPat1/2020 strain. We thank Dr. Shai Weiss for safety advisory. We thank Dr. Michal Mandelboim for MDCK cells and Influenza virus A/Puerto Rico/8/34 H1N1 (PR8).

Author contributions

H.A, E.B.V, B.P, S.M, T.I designed the research; H.A, E.B.V, B.P, S.M, R.A, H.T, Y.Y.R, N.E, L.C.M, Y.V, D.G, E.M, N.P, and T.I, performed the experiments. H.A, E.B.V. N.P, T.I wrote the manuscript. All authors discussed results and commented on the manuscript before submission. R.A. is supported by the Israel Science Foundation (grant 521/18). E.B.V is supported by the Katzir Foundation.

Competing interests

The author declare no conflict of interest.

References

1. https://www.who.int/emergencies/diseases/novel-coronavirus-2019. World Health Organization Coronavirus Disease (COVID-19) pandemic. (2020).
2. Regina, J., *et al.* Epidemiology, risk factors and clinical course of SARS-CoV-2 infected patients in a Swiss university hospital: An observational retrospective study. *PLOS ONE* **15**, e0240781 (2020).
3. https://www.cdc.gov/flu/about/burden/index.html. Centers for Disease Control and Prevention. Influenza (Flu). (2020).
4. McCullers, J.A. The co-pathogenesis of influenza viruses with bacteria in the lung. *Nature Reviews Microbiology* **12**, 252-262 (2014).
5. Falsey, A.R., *et al.* Bacterial complications of respiratory tract viral illness: a comprehensive evaluation. *The Journal of infectious diseases* **208**, 432-441 (2013).
6. Oladunni, F.S., *et al.* Lethality of SARS-CoV-2 infection in K18 human angiotensin-converting enzyme 2 transgenic mice. *Nature Communications* **11**, 6122 (2020).
7. Blazejewska, P., *et al.* Pathogenicity of different PR8 influenza A virus variants in mice is determined by both viral and host factors. *Virology* **412**, 36-45 (2011).
8. Nickbakhsh, S., *et al.* Virus–virus interactions impact the population dynamics of influenza and the common cold. *Proceedings of the National Academy of Sciences* **116**, 27142-27150 (2019).
9. Wolff, G.G. Influenza vaccination and respiratory virus interference among Department of Defense personnel during the 2017–2018 influenza season. *Vaccine* **38**, 350-354 (2020).
10. Rigby, R.E., Wise, H.M., Smith, N., Digard, P. & Rehwinkel, J. PA-X antagonises MAVS-dependent accumulation of early type I interferon messenger RNAs during influenza A virus infection. *Scientific Reports* **9**, 7216 (2019).
11. Felgenhauer, U., *et al.* Inhibition of SARS-CoV-2 by type I and type III interferons. *The Journal of biological chemistry* **295**, 13958-13964 (2020).

12. McAfee, M.S., Huynh, T.P., Johnson, J.L., Jacobs, B.L. & Blattman, J.N. Interaction between unrelated viruses during in vivo co-infection to limit pathology and immunity. *Virology* **484**, 153-162 (2015).
13. Huang, I.-C.*, et al.* Influenza A Virus Neuraminidase Limits Viral Superinfection. *Journal of Virology* **82**, 4834-4843 (2008).
14. Vagima, Y.*, et al.* Influenza virus infection augments susceptibility to respiratory Yersinia pestis exposure and impacts the efficacy of antiplague antibiotic treatments. *Scientific Reports* **10**, 19116 (2020).
15. Israely, T.*, et al.* Differential Response Following Infection of Mouse CNS with Virulent and Attenuated Vaccinia Virus Strains. *Vaccines* **7**(2019).
16. Yahalom-Ronen, Y.*, et al.* A single dose of recombinant VSV-ΔG-spike vaccine provides protection against SARS-CoV-2 challenge. *Nature Communications* **11**, 6402 (2020).

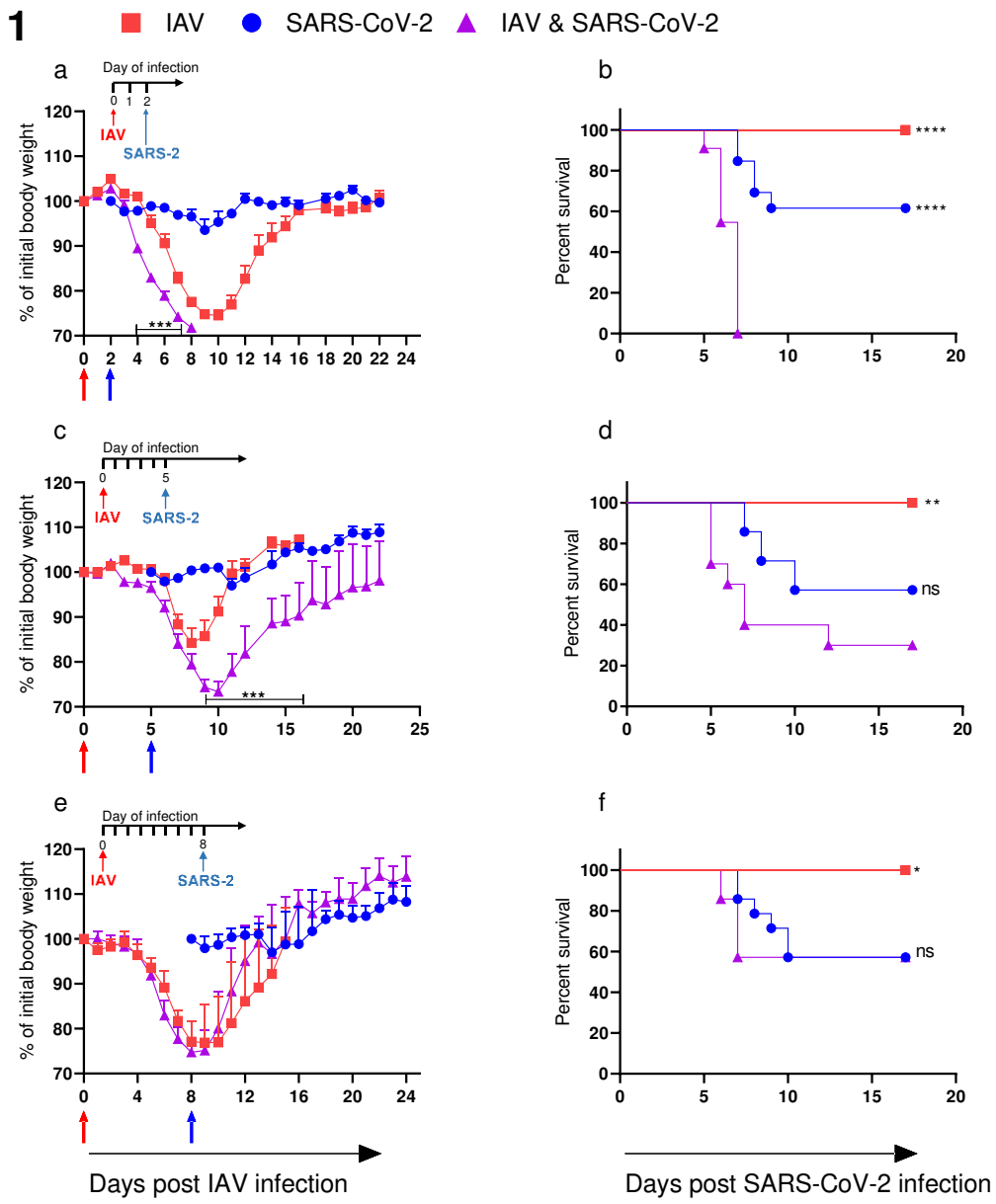

Fig. 1: Morbidity and mortality in K18-hACE2 mice infected with SARS-CoV-2 following influenza infection

K18-hACE2 mice were infected with IAV (80 pfu/mice, i.n), followed by infection with SARS-CoV-2 (10 pfu/mice, i.n) at two (a,b), five (c,d) or eight (e,f) dpIi. Percent body weight loss following infection (a,c,e). Red arrow represents IAV infection. Blue arrow represents SARS-CoV-2 infection. Error bars represent standard errors (SE). p.values are indicated in the figure as asterisks, and were calculated by Student's t-test using GraphPad Prism 8.4.3. ***p<0.0002 at 4-7 dpIi (a), and at 9-16 dpIi (c) IAV infection compared to co-infection. Survival curves (b,d,f):

*p=0.04; **p=0.0026; ****p<0.0001 IAV or SARS-CoV-2 infection compared to co-infected. ns, not significant, Log-rank (Mantel-Cox). Figure shows one representative experiment out of 4 (a,b), 2 (c,d), 1 (e,f) performed. Figure shows: IAV infected group consists of 10 (a,b), 11 (c,d) or 8 (e,f) mice. SARS-CoV-2 infected group consists of 13 (a,b) or 14 (c-f) mice. Co-infection group consists of 11 (a,b), 10 (c,d) or 7 (e,f) mice.

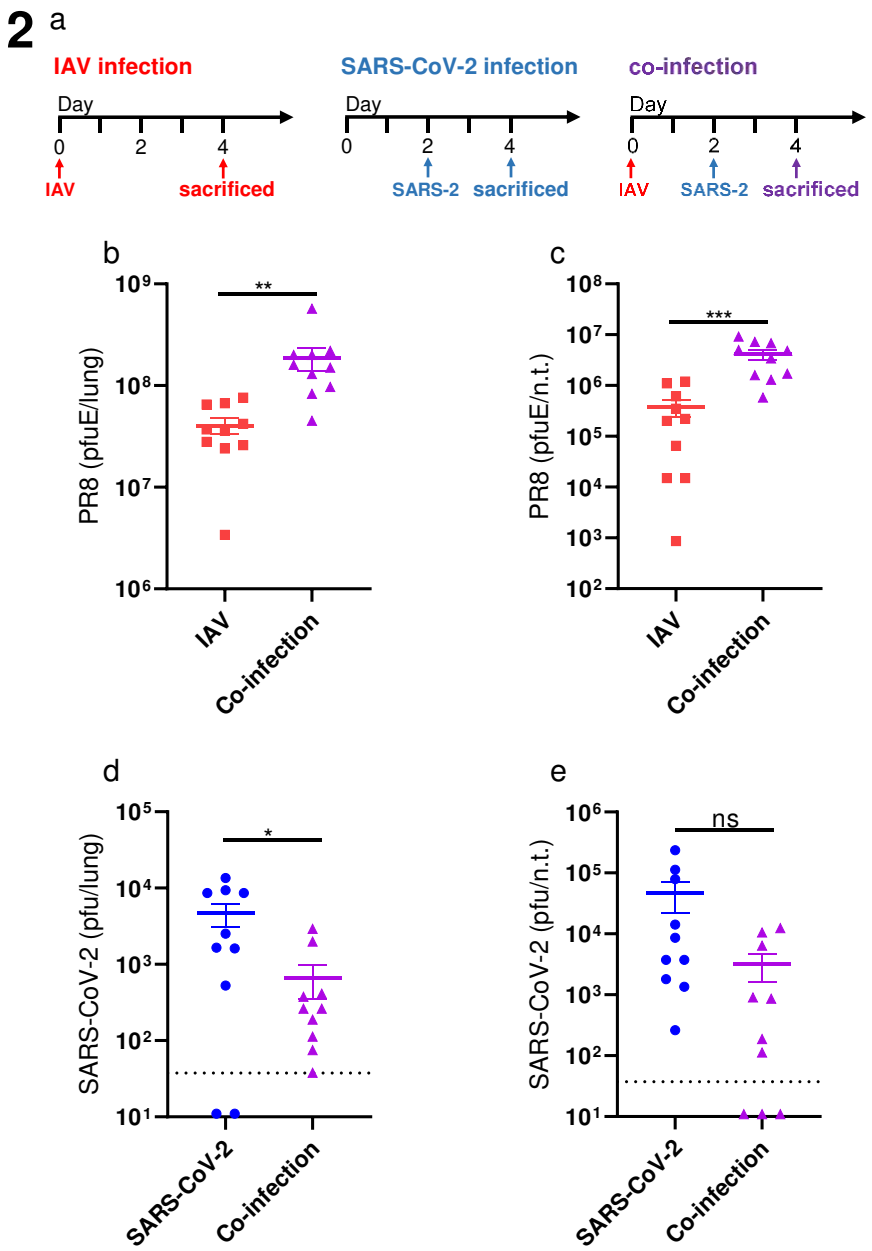

297

298 **Fig. 2: Increased IAV and decreased SARS-CoV-2 viral load in co-infected mice**

299 (a) Schematic time lines, K18-hACE2 mice were sacrificed at 4 dpIi and 2 dpSi. IAV viral RNA
300 load was measured in lungs (b) and nasal turbinates (n.t), (c) and the pfu Equivalent per organ
301 (pfuE/organ) were calculated. SARS-CoV-2 viral load was determined by pfu in lungs (d) and in
302 nasal turbinates (e).

303 Each symbol represents one mouse (10 mice each group). Lines represent mean. Error bars
304 represent SE. *p=0.0212; **p=0.0062; ***p=0.0008, ns, not significant, Student's t-test.

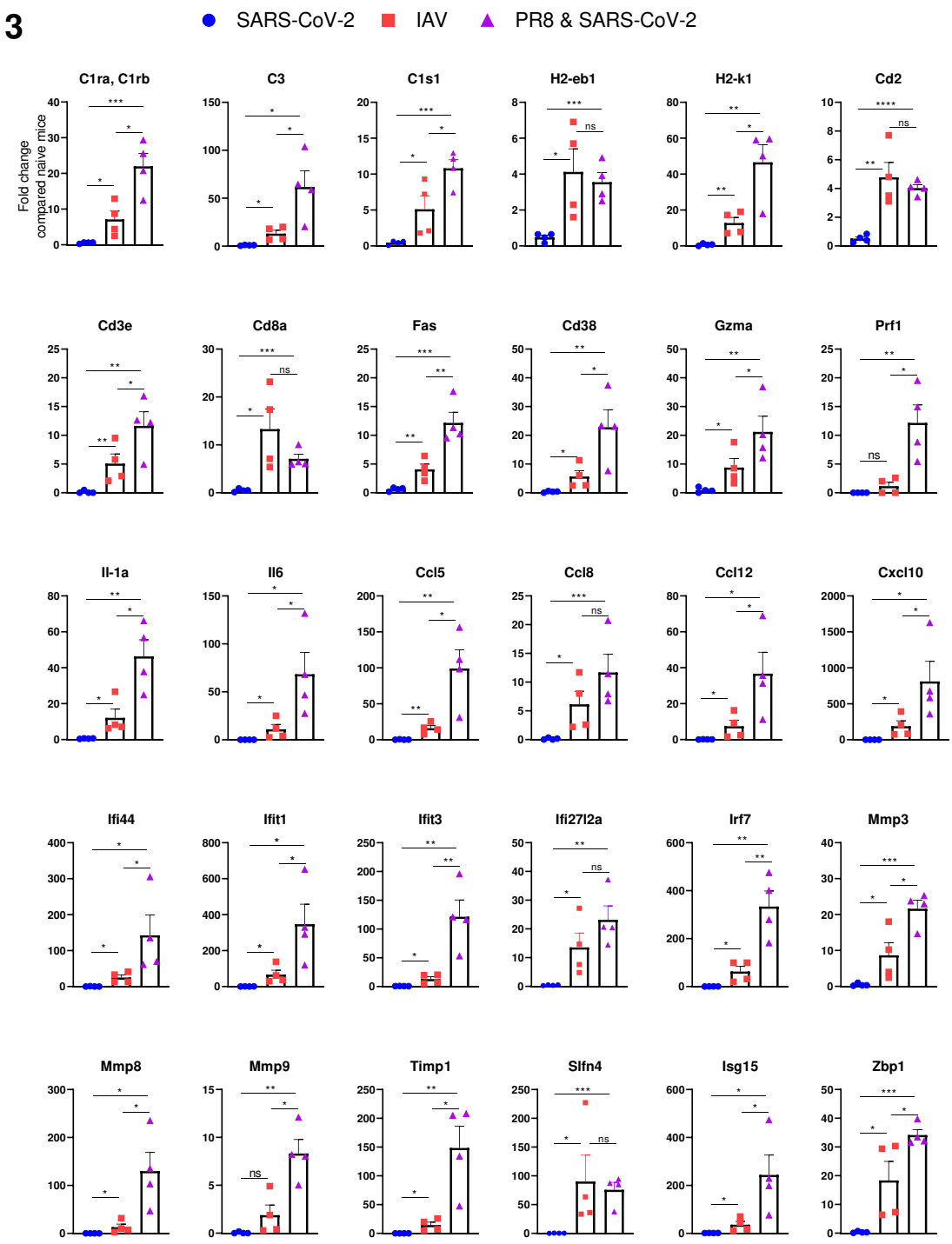

Fig. 3: A panel of increased inflammatory-related genes in the lungs of co-infected mice

Expression of various inflammatory related genes in the lungs. RNA were isolated from lungs of K18-hACE2 mice 4 dpIi or 2 dpSi and analyzed by quantitative real-time RT-PCR. Each symbol represents one mouse (4 per each group). Y axis represents fold change of infected compared to

naïve mice. Colum height represent mean. Error bars represent SE. *p<0.05; **p<0.005; ***p<0.0005 Student's t-test. The genes tested can be divided to different groups: complement system (C1ra, C1rb, C3 and C1s1); antigen presentation (H2-eb1 and H2-k1); recruitment and activation of immune cells (Cd2, Cd3e, Cd8a, Fas, Cd38, Gzma, Prf1); interleukins (Il) (Il-1a and Il6); chemokines (Ccl5, Ccl8, Ccl12, Cxcl10); interferon (Ifi44, Ifit1, Ifit3, Ifi27l2a, Irf7); matrix metalloproteinase (Mmp) and tissue damage (Mmp3, Mmp8, Mmp9, Timp1); and a members of the Schlafen (Slfn) family, Slfn4 and the ubiquitin-like modifier Isg15 and Z-DNA binding protein 1 (Zbp1).

4

Symbol	SARS-CoV-2 Pre-immune	Infection with	n
	Yes	SARS-CoV-2	7
	No	IAV	7
	No	SARS-CoV-2	9
	Yes	IAV & SARS-CoV-2	14
	No	IAV & SARS-CoV-2	9

Symbol	IAV Pre-immune	Infection with	n
	Yes	IAV	5
	No	IAV	7
	Yes	IAV & SARS-CoV-2	9
	No	SARS-CoV-2	9
	Yes	SARS-CoV-2	8
	No	IAV & SARS-CoV-2	9

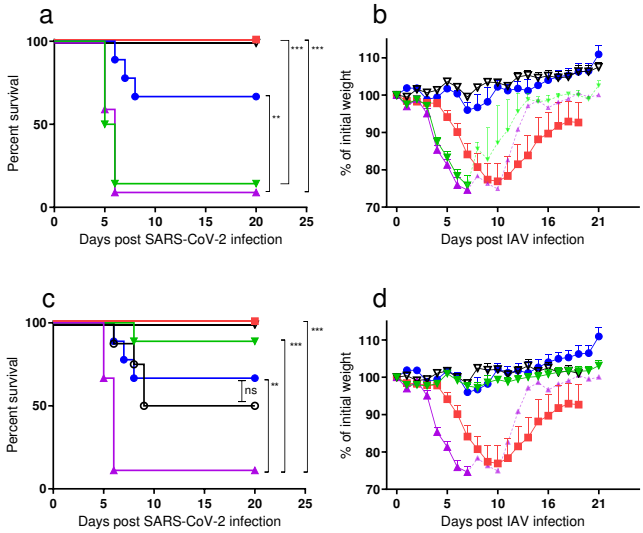

Fig. 4: Prior immunity to IAV, but not to SARS-CoV-2, rescue co-infected K18-hACE2 mice K18-hACE2 mice were immunized to SARS-CoV-2 by infection with 2pfu/mouse SARS-CoV-2 (a,b), or immunized to IAV by 10^6pfu/mouse IAV (i.m.) (c,d). Thirty days post immunization, pre-immunized and non-immunized mice were infected i.n. with the indicated virus. Survival curves (a,c): **p=0.0024; ***P<0.0006. ns, not significant, Log-rank (Mantel-Cox). Percent of weight loss following infection (b,d). Error bars represent SE. Figure legend is shown in tables. n, number of mice in each group. Dashed lines (b,d) represent 1 or 2 survived mice out of 9 or 14, respectively.

Figures

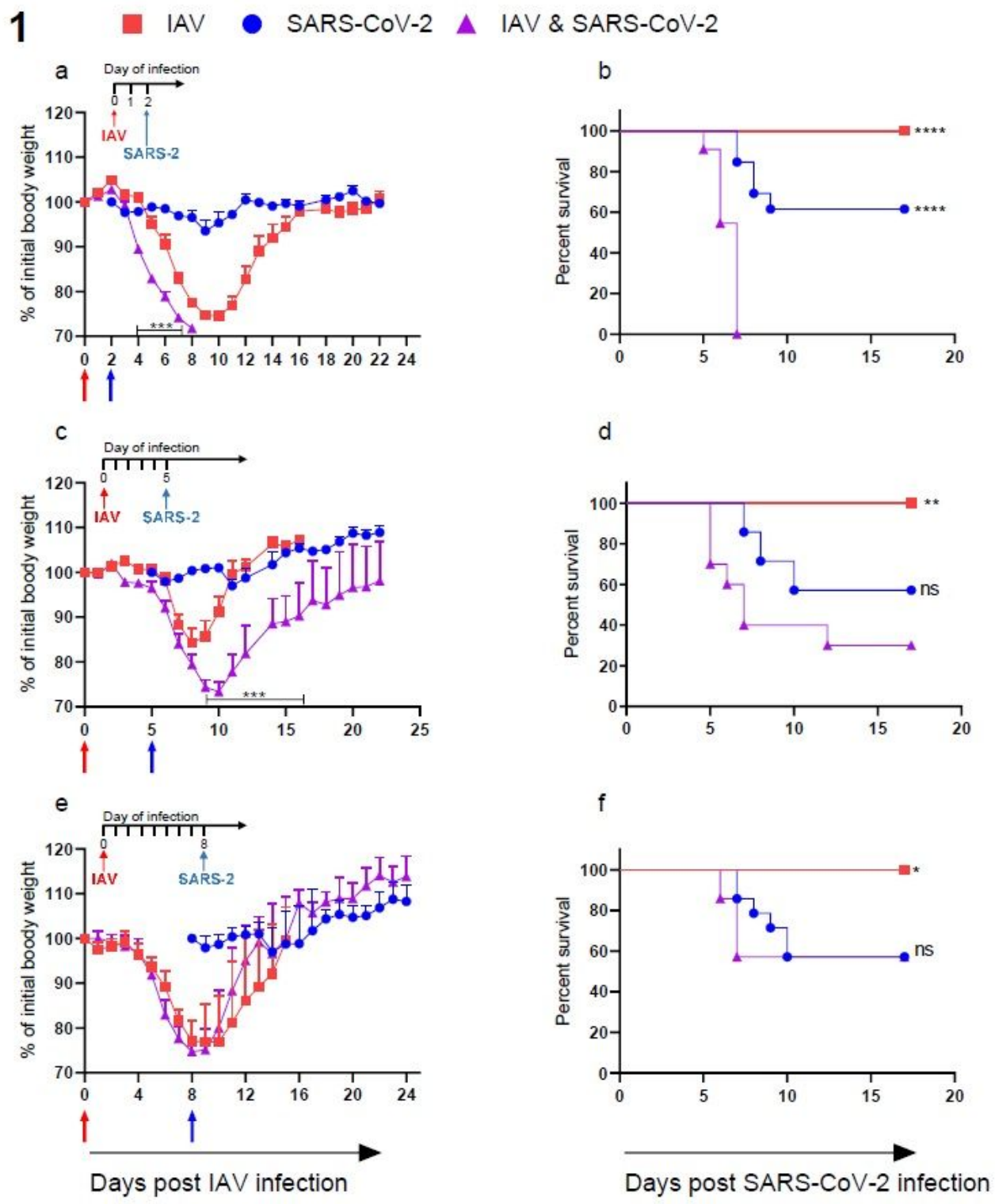

Figure 1

Morbidity and mortality in K18-hACE2 mice infected with SARS-CoV-2 following influenza infection K18-hACE2 mice were infected with IAV (80 pfu/mice, i.n), followed by infection with SARS CoV-2 (10 pfu/mice, i.n) at two (a,b), five (c,d) or eight (e,f) dpli. Percent body weight loss following infection (a,c,e).

Red arrow represents IAV infection. Blue arrow represents SARS-CoV-2 infection. Error bars represent standard errors (SE). p.values are indicated in the figure as asterisks, and were calculated by Student's t-test using GraphPad Prism 8.4.3. ***p<0.0002 at 4-7 dpli (a), and at 9-16 dpli (c) IAV infection compared to co-infection. Survival curves (b,d,f):*p=0.04; **p=0.0026; ****p<0.0001 IAV or SARS-CoV-2 infection compared to co-infected. ns, 291 not significant, Log-rank (Mantel-Cox). Figure shows one representative experiment out of 4 (a,b), 292 2 (c,d), 1 (e,f) performed. Figure shows: IAV infected group consists of 10 (a,b), 11 (c,d) or 8 (e,f) 293 mice. SARS-CoV-2 infected group consists of 13 (a,b) or 14 (c-f) mice. Co-infection group consists 294 of 11 (a,b), 10 (c,d) or 7 (e,f) mice.

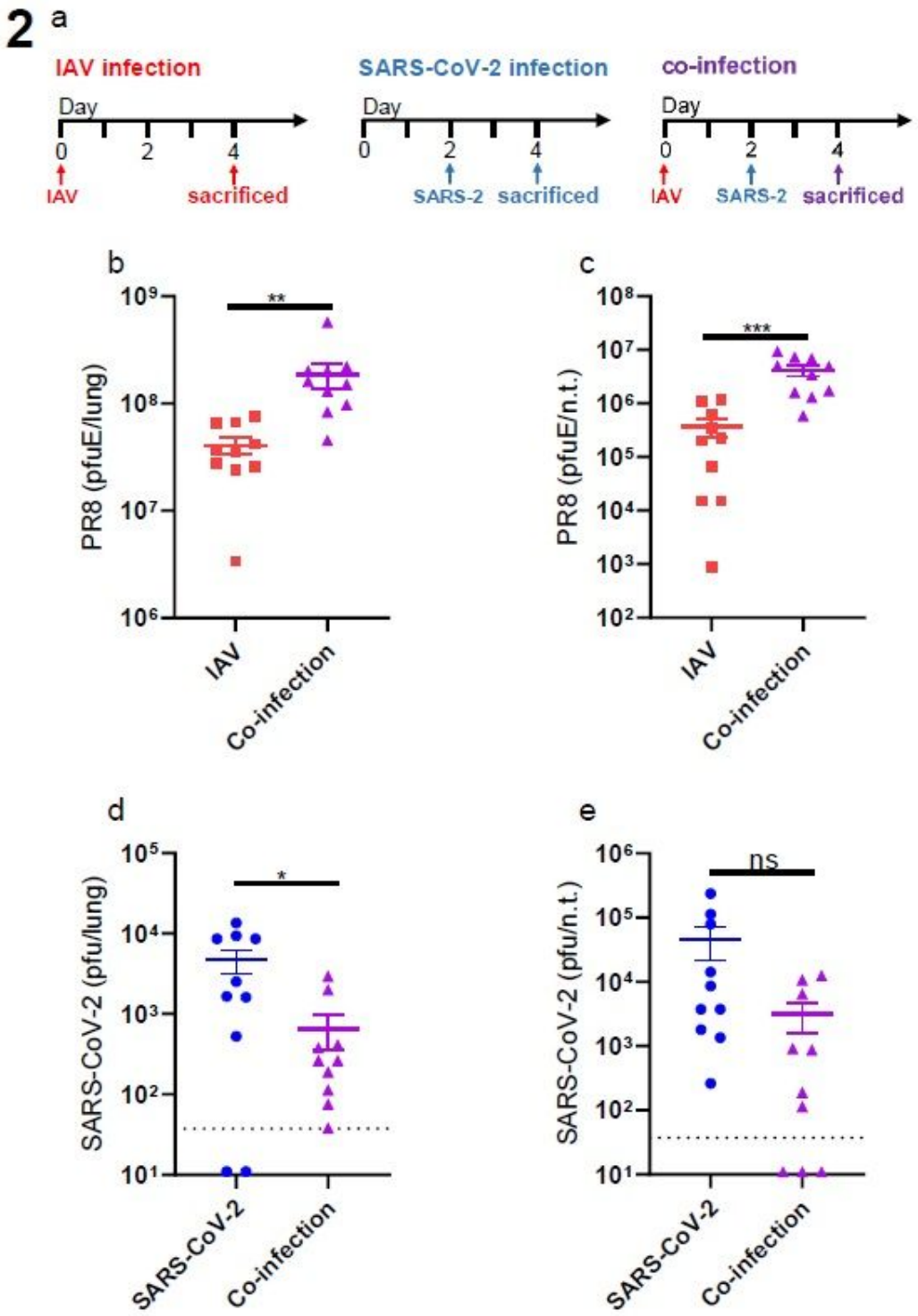

Figure 2

Increased IAV and decreased SARS-CoV-2 viral load in co-infected mice (a) Schematic time lines, K18-hACE2 mice were sacrificed at 4 dpIi and 2 dpSi. IAV viral RNA load was measured in lungs (b) and nasal turbinates (n.t), (c) and the pfu Equivalent per organ (pfuE/organ) were calculated. SARS-CoV-2 viral load was determined by pfu in lungs (d) and in nasal turbinates (e). Each symbol represents one mouse (10

mice each group). Lines represent mean. Error bars represent SE. *p=0.0212; **p=0.0062; ***p=0.0008, ns, not significant, Student's t-test.

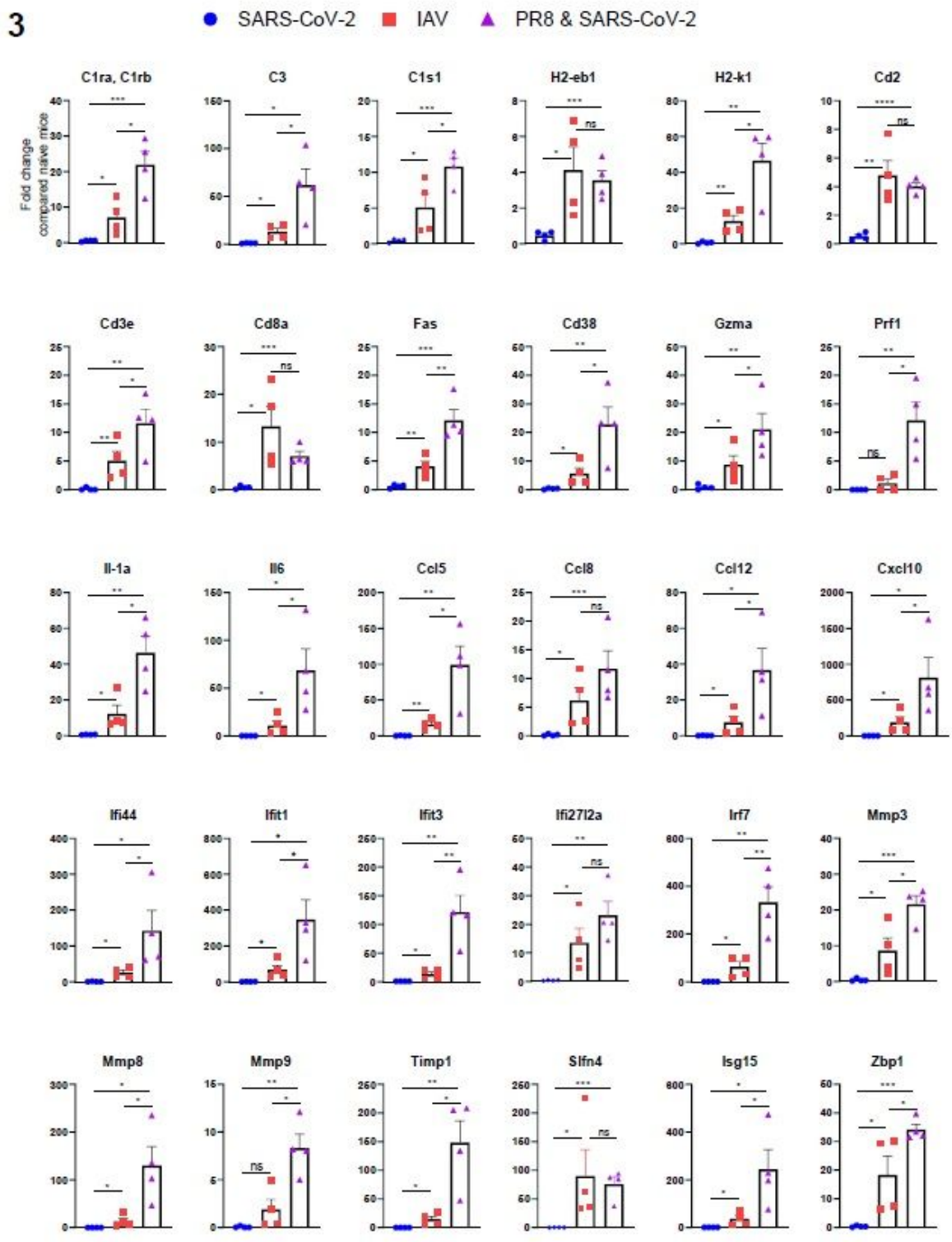

Figure 3

A panel of increased inflammatory-related genes in the lungs of co-infected mice Expression of various inflammatory related genes in the lungs. RNA were isolated from lungs of K18-hACE2 mice 4 dpli or 2 dpSi and analyzed by quantitative real-time RT-PCR. Each symbol represents one mouse (4 per each

group). Y axis represents fold change of infected compared to naïve mice. Colum height represent mean. Error bars represent SE. *p<0.05; **p<0.005; 310 ***p<0.0005 Student's t-test. The genes tested can be divided to different groups: complement 311 system (C1ra, C1rb, C3 and C1s1); antigen presentation (H2-eb1 and H2-k1); recruitment and 312 activation of immune cells (Cd2, Cd3e, Cd8a, Fas, Cd38, Gzma, Prf1); interleukins (Il) (Il-1a and Il6); chemokines (Ccl5, Ccl8, Ccl12, Cxcl10); interferon (Ifi44, Ifit1, Ifit3, Ifi27l2a, Irf7); matrix metalloproteinase (Mmp) and tissue damage (Mmp3, Mmp8, Mmp9, Timp1); and a members of the Schlafen (Slfn) family, Slfn4 and the ubiquitin-like modifier Isg15 and Z-DNA binding 3 protein 1 (Zbp1).

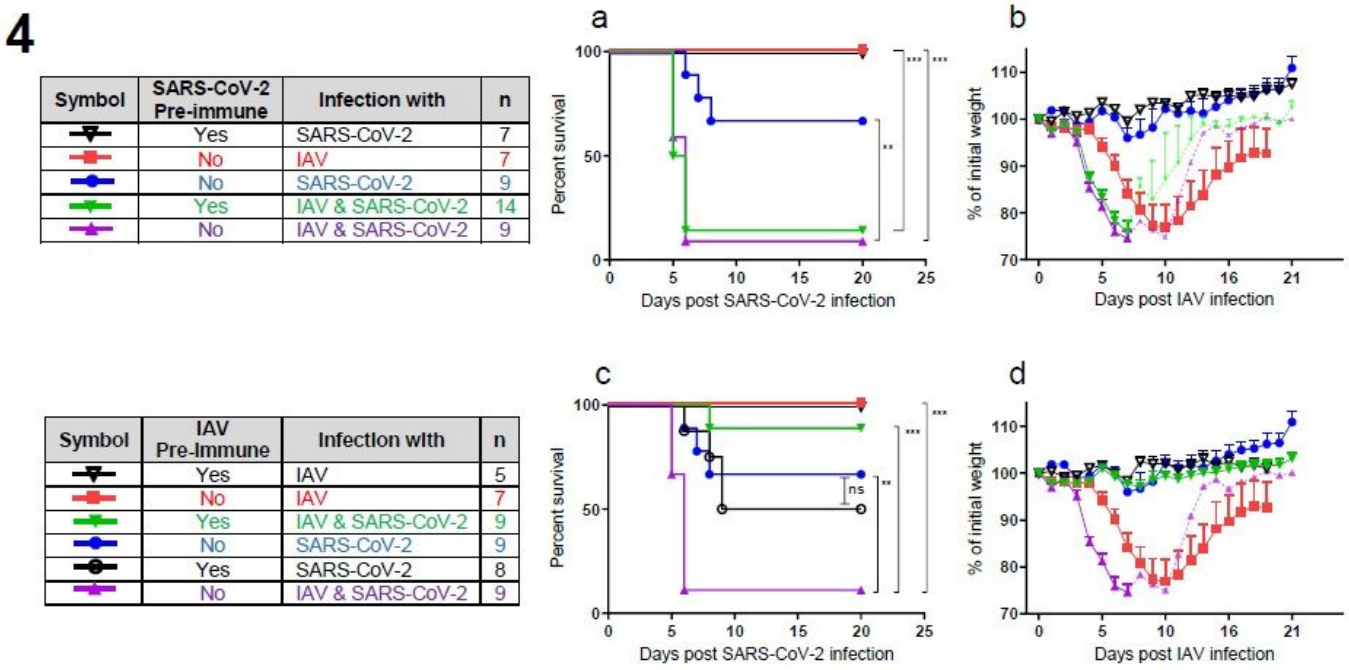

Figure 4

Prior immunity to IAV, but not to SARS-CoV-2, rescue co-infected K18-hACE2 mice K18-hACE2 mice were immunized to SARS-CoV-2 by infection with 2pfu/mouse SARS-CoV-2 (a,b), or immunized to IAV by 106pfu/mouse IAV (i.m.) (c,d). Thirty days post immunization, preimmunized and non-immunized mice were infected i.n. with the indicated virus. Survival curves (a,c): **p=0.0024; ***P<0.0006. ns, not significant, Log-rank (Mantel-Cox). Percent of weight loss following infection (b,d). Error bars represent SE. Figure legend is shown in tables. n, number of mice in each group. Dashed lines (b,d) represent 1 or 2 survived mice out of 9 or 14, respectively.